

Method for distinguishing between ordered and chaotic orbits in four-dimensional maps

N. Voglis, G. Contopoulos, and C. Efthymiopoulos

Department of Astronomy, University of Athens, Panepistimiopolis, GR 157 84-Athens, Greece

(Received 15 July 1997; revised manuscript received 2 September 1997)

The usual methods for distinguishing ordered and chaotic orbits in three-dimensional (3D) Hamiltonian systems, or 4D maps, are either inefficient (because we cannot visualize 4D figures), or slow (e.g., the calculation of Lyapunov characteristic numbers). Here we provide an efficient and fast method, based on the spectra of stretching numbers (short-time Lyapunov characteristic numbers), or helicity angles (angles of infinitesimal deviations from an orbit with a fixed direction). *The spectra for two different initial deviations are the same for chaotic orbits, but different for ordered orbits.* We apply this method to a difficult case of weak chaos (small Lyapunov characteristic number), and prove its advantages with respect to other methods. Finally we explain the different behavior of ordered and chaotic orbits theoretically. [S1063-651X(98)08801-1]

PACS number(s): 05.45.+b, 46.10.+z

I. INTRODUCTION

The distinction between ordered and chaotic motions is particularly difficult in systems of three degrees of freedom, because we cannot visualize a four-dimensional (4D) Poincaré surface of section. Of course one can make such a distinction by calculating the Lyapunov characteristic numbers \mathcal{L} of each orbit. But this method is very time consuming, because one usually needs very long calculations. Furthermore the evaluation of \mathcal{L} sometimes may lead to uncertain answers because of the effect of stickiness. Thus a faster method based on short-time calculations is urgently needed.

In two recent papers [1,2], we discussed the spectra of ‘‘stretching numbers’’ and ‘‘helicity angles’’ of ordered and chaotic orbits in systems of two- and three-degrees of freedom. Consider an initial condition \mathbf{x}_0 on the Poincaré surface of section and an initial deviation ξ_0 from \mathbf{x}_0 . Let their respective Poincaré map iterates be \mathbf{x}_i and ξ_i , $i=1,2,3,\dots$. The stretching number is the logarithm of the ratio of the infinitesimal deviations $|\xi_i|$ and $|\xi_{i+1}|$, at successive points \mathbf{x}_i and \mathbf{x}_{i+1} ,

$$a_i = \ln \frac{|\xi_{i+1}|}{|\xi_i|}. \quad (1)$$

This is, in fact, a short-time (period-1) Lyapunov characteristic number. Short-time Lyapunov characteristic numbers have been used by several authors since 1983 [3–8]. In particular period-1 Lyapunov characteristic numbers were introduced by Froeschlé, Froeschlé, and Lohinger [9] and Voglis and Contopoulos [1].

On the other hand, the helicity angle in a system of two-degrees of freedom is the angle ϕ_i between an infinitesimal deviation ξ_i with a fixed direction, e.g., the x axis.

In the case of a 4D map x_i ($i=1, 2, 3$, and 4) on a Poincaré surface of section we define three helicity angles, e.g., the angles ϕ_{1i} , ϕ_{2i} , and ϕ_{4i} of the projection of the vector ξ_i on the planes (x_1, x_3) , (x_2, x_3) , and (x_4, x_3) with the axis x_3 .

The spectra of stretching numbers and helicity angles are the distributions of the a 's and ϕ 's. The spectra of different chaotic orbits in a connected chaotic domain are invariant,

i.e. independent of the initial condition \mathbf{x}_0 and of the initial deviation ξ_0 . On the other hand, the spectra of ordered orbits depend on the initial conditions \mathbf{x}_0 and deviations ξ_0 . In the present paper we study this difference between chaotic and ordered spectra, which gives an easy and efficient method to distinguish between ordered and chaotic motion.

II. TWO COUPLED STANDARD MAPS

We consider the case of two coupled standard maps:

$$\begin{aligned} x'_1 &= x_1 + x'_2, \\ x'_2 &= x_2 + \frac{K}{2\pi} \sin 2\pi x_1 - \frac{\beta}{\pi} \sin 2\pi(x_3 - x_1), \\ x'_3 &= x_3 + x'_4 \pmod{1}, \\ x'_4 &= x_4 + \frac{K}{2\pi} \sin 2\pi x_3 - \frac{\beta}{\pi} \sin 2\pi(x_1 - x_3), \end{aligned} \quad (2)$$

where K is the nonlinearity parameter and β the coupling constant.

We take $K=3$ and various values of β . For $\beta=0$ the maps (x_1, x_2) and (x_3, x_4) are uncoupled. Each map contains a large island of stability embedded in a chaotic sea (Fig. 1). Most chaotic orbits, like orbit (1), fill the chaotic sea, while ordered orbits, like orbit (3), form invariant curves in the island of stability.

If $\beta=0.1$ the orbit (x_1, x_2, x_3, x_4) with the initial conditions of orbit (1) is projected on the plane (x_1, x_2) almost completely ergodically [Fig. 2(a)]. The same is true with the projections on the planes (x_1, x_3) , (x_1, x_4) , (x_2, x_3) , (x_2, x_4) , and (x_3, x_4) .

The finite time Lyapunov characteristic number

$$\mathcal{L}_t = \frac{\ln(|\xi|/|\xi_0|)}{t} \quad (3)$$

for this orbit is given as a function of $\log_{10} t$ in Fig. 2(b), where t is a discrete time, i.e., the number of iterations of the

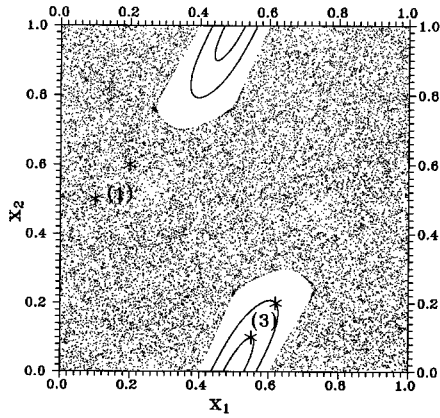


FIG. 1. The map (x_1, x_2) for $K=3$ and $\beta=0$. The chaotic orbit (1) (initial conditions $x_1=0.1$, $x_2=0.5$, $x_3=0.2$, and $x_4=0.6$) fills most of the square (x_1, x_2) and the same region in the (x_3, x_4) plane. The ordered orbit (3) (initial conditions $x_1=0.55$, $x_2=0.1$, $x_3=0.62$, and $x_4=0.2$) forms invariant curves on both planes (x_1, x_2) and (x_3, x_4) . The initial conditions (x_1, x_2) and (x_3, x_4) of both orbits are marked as stars.

map (2). The direction of the (very small) initial deviation ξ is given by the ratios $z_k = \xi_{k0}/\xi_{30}$, $k=1, 2, 3$, and 4, where z_3 is always 1.

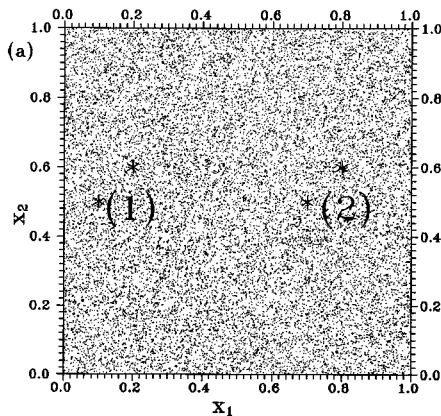
The usual Lyapunov characteristic number

$$\mathcal{L} = \lim_{t \rightarrow \infty} \mathcal{L}_t \quad (4)$$

is about $\mathcal{L}=0.75$. We see that this value is reached approximately after 10^4 iterations. However, for smaller times t the values of \mathcal{L}_t vary considerably.

Another orbit in the same chaotic domain [orbit (2) in Fig. 2(a)] gives the same limit $\mathcal{L}=0.75$ after about $t=10^4$ iterations. However, the variations of \mathcal{L}_t for smaller t are very different from those of the original orbit (1).

On the other hand if we take the same orbit (1) but a different initial deviation we find essentially the same variations of \mathcal{L}_t after an initial transient period of only about $t=10$ iterations [the solid line close to orbit (1) in Fig. 2(b)].



Similarly, a different initial deviation from orbit (2) gives the same variations of \mathcal{L}_t as orbit (2), after a short initial transient period [the dashed line close to orbit (2) in Fig. 2(b)].

The spectra of stretching numbers a , and helicity angles ϕ_1 of orbit (1) for a deviation $z_1=z_2=z_3=z_4=1$, and 10^4 iterations are shown in Figs. 3(a) and 3(b). The spectra for deviations $z_1=z_2=2$ and $z_3=z_4=1$ are shown as dots. We see that, after $t=10^4$ iterations, the spectra for the same orbit but different deviations are exactly the same. The same is true for orbit (2). However, orbits (1) and (2) with the same deviations z_k give somewhat different spectra after 10^4 iterations [Fig. 3(c)]. But if we extend our calculations for 10^5 iterations [Fig. 3(d)], the spectra are almost identical. In fact the two spectra tend to the same invariant spectrum of the large chaotic sea. The same phenomena appear for the helicity angles ϕ_2 and ϕ_4 .

In contrast to the above chaotic orbits, the spectra of ordered orbits are different, not only for different orbits, but also for different deviations from a given orbit. This is seen in the spectra of Figs. 4(b) and 4(c), that correspond to the same constants $K=3$ and $\beta=0.1$ as the previous orbits, but initial conditions $x_1=0.55$, $x_2=0.1$, $x_3=0.62$, and $x_4=0.2$ [orbit (3)]. The points (x_1, x_2) and (x_3, x_4) both belong to the island of stability of Fig. 1, and define an invariant curve on each plane. When the coupling constant is $\beta=0.1$ the orbit on the plane (x_1, x_2) fills a ring [Fig. 4(a)]. This is not due to diffusion, but to a projection of a toroidal surface.

The spectra of stretching numbers a and helicity angles ϕ_1 for initial deviations $z_1=z_2=z_3=z_4=1$ and $t=10^5$ iterations are given as solid lines in Figs. 4(b) and 4(c), while the spectra for initial deviations $z_1=z_2=2$ and $z_3=z_4=1$ are given as dashed lines. We see that the two spectra are quite different.

On the other hand, the spectra along each orbit (with the same initial deviation) are invariant. In fact, if we take the last $t=10^5$ periods out of a total of $t=10^9$ periods, we find exactly the same spectra as for the first 10^5 periods [dots in Figs. 4(b) and 4(c)]. Thus we see that the spectra of chaotic orbits are independent of the initial deviations from the same orbit, while the spectra of ordered orbits are different for different initial deviations from the same orbit.

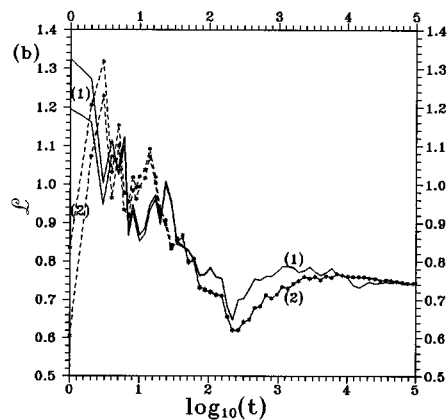


FIG. 2. (a) The projection of map (2) on the plane (x_1, x_2) for $K=3$ and $\beta=0.1$. The initial conditions of orbits (1) ($x_1=0.1$, $x_2=0.5$, $x_3=0.2$, and $x_4=0.6$) and (2) ($x_1=0.8$, $x_2=0.6$, $x_3=0.7$, and $x_4=0.5$) are marked. Both orbits give essentially the same distribution of points. (b) The finite-time Lyapunov characteristic number as a function of $\log_{10}(t)$, where t is the time (number of iterations) for orbit (1) and two initial deviations: $z_1=z_2=z_3=z_4=1$ and $z_1=z_2=2$, $z_3=z_4=1$ (upper and lower solid lines), and for orbit (2) and the same initial deviations (lower and upper dashed lines).

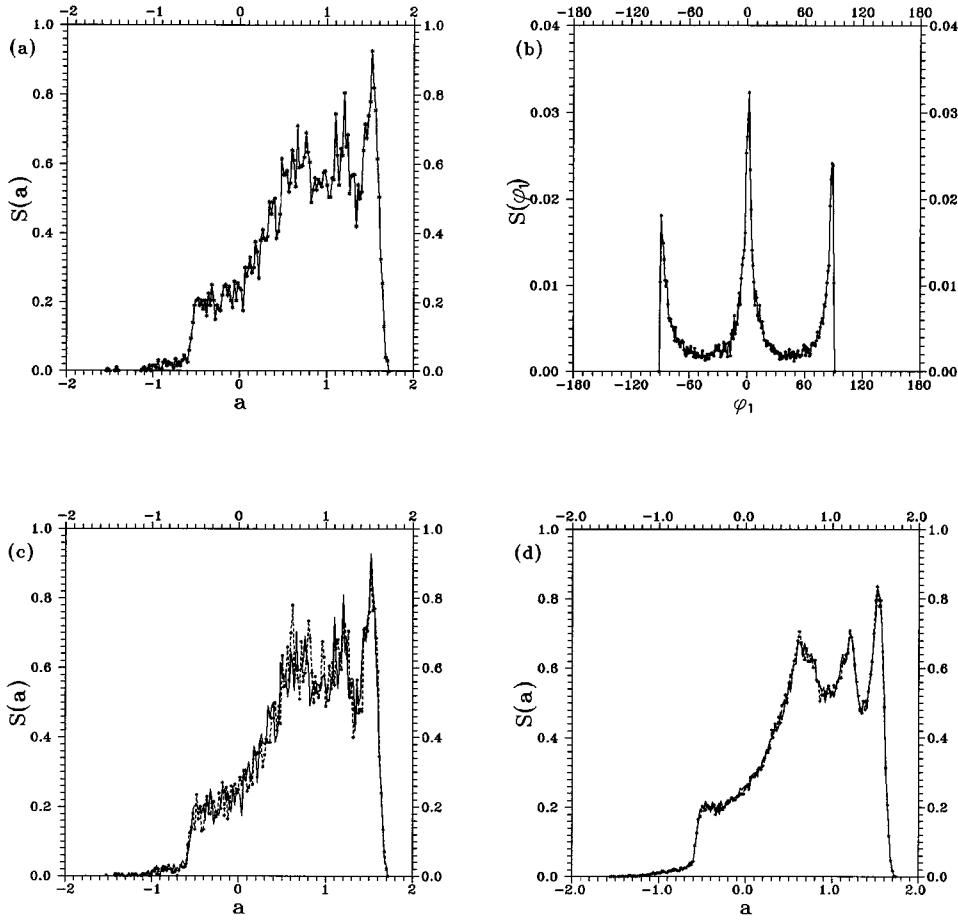


FIG. 3. The spectra of (a) stretching numbers a , and (b) helicity angles ϕ_1 for orbit (1) calculated for $t=10^4$ iterations with initial deviations $z_1=z_2=z_3=z_4=1$ (solid line) and $z_1=z_2=2, z_3=z_4=1$ (dots). (c) The spectra of stretching numbers for the orbits (1) (solid line) and (2) (dashed line) for the same initial deviations, calculated for $t=10^4$ iterations. (d) The same spectra calculated for $t=10^5$ iterations.

Our method can distinguish between ordered and chaotic orbits after a much shorter time than needed to calculate the Lyapunov characteristic numbers. For example in the case of the chaotic orbits of Fig. 2(b), the time required to stabilize \mathcal{L} is 10^4-10^5 periods, while for ordered orbits \mathcal{L} decreases almost like t^{-1} . But the closeness or significant difference of two spectra with the same initial conditions and different deviations ξ can be established well before the spectra have reached their final form, e.g., after only 5×10^2 periods [Figs. 5(a) and 5(b)]. In the chaotic case [Fig. 5(a)] the two deviations give almost identical spectra, while in the ordered case the differences are quite significant [Fig. 5(b)]. On the

other hand, the computational cost in calculating the spectra is practically the same as that needed to calculate \mathcal{L} for the same time, because both require the integration of the variational equations.

In order to check this method further, we now study an orbit that shows only a little chaos, after a long time. This is an orbit [Fig. 6(a)] with the same $K=3$ and the same initial conditions as in Fig. 4, but with $\beta=0.3051$ instead of $\beta=0.1$. This orbit fills a region [Fig. 6(a)] similar to that of Fig. 4(a). However its spectra, calculated for 10^5 periods, are very different [Figs. 6(b) and 6(c)] from the spectra with $\beta=0.1$ [compare Figs. 6(b) and 6(c) with Figs. 4(b) and 4(c)].

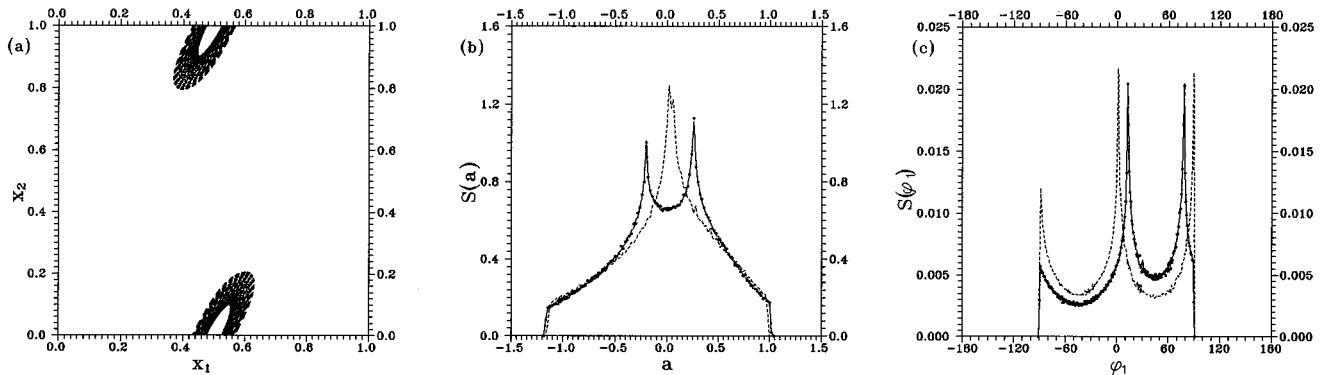


FIG. 4. (a) The regular orbit (3) for $K=3$ and $\beta=0.1$ (initial conditions in Fig. 1), calculated for 10^5 iterations, projected on the plane (x_1, x_2) . The spectra of (b) stretching numbers and (c) helicity angles ϕ_1 , for $t=10^5$ iterations and initial deviations $z_1=z_2=z_3=z_4=1$ (solid line) and $z_1=z_2=2, z_3=z_4=1$ (dashed lines). The two spectra of each figure are quite different. The dots in (b) and (c) represent the spectra of the last 10^5 iterations out of 10^9 iterations.

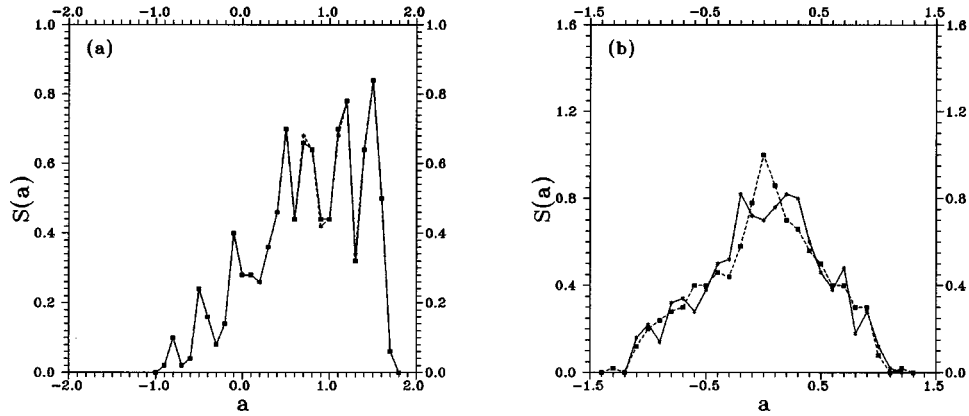


FIG. 5. The spectra of stretching numbers for $t=5 \times 10^2$ iterations and initial deviations $z_1=z_2=z_3=z_4=1$ (solid line) and $z_1=z_2=2, z_3=z_4=1$ (dashed line) for (a) the chaotic orbit (1) [Fig. 2(a)] and (b) the ordered orbit (3) [Fig. 4(a)].

The spectra shown by solid and dashed lines in Figs. 6(b) and 6(c) correspond to different deviations, and they are only slightly different, and, as the integration time increases, their differences tend to zero. This is seen in Fig. 7 which gives the spectra of α and φ_1 for 2×10^6 iterations.

The distinction between the ordered spectra of Fig. 4 and the chaotic spectra of Fig. 6 is remarkable because the two orbits look quite similar. Furthermore, the finite time Lyapunov characteristic numbers of the two orbits (Fig. 8) are very close to each other for $10^2 < t < 10^8$, decreasing roughly linearly in a logarithmic scale, $\log_{10}(\mathcal{L}_t)$ versus $\log_{10}t$, along a line parallel to the diagonal. This is consistent with a power deviation $\xi = ct^p + \xi_0$, characteristic of an ordered orbit. In fact in such a case the values of $\log_{10}\mathcal{L}_t$ tend to vary like $-\log_{10}t$. However, after $t=10^8$ iterations the values of \mathcal{L}_t in the case $\beta=0.3051$ tend to stabilize at a limiting value $\mathcal{L}=4 \times 10^{-7}$, while in the case $\beta=0.1$ the values of \mathcal{L}_t decrease, in the same way as before, toward zero.

We conclude that the distinction between the ordered orbit ($\beta=0.1$) and the chaotic orbit ($\beta=0.3051$) requires about $t=10^9$ iterations if we use the criterion of the Lyapunov characteristic number, while it can be seen after only 10^5 iterations (or even less) if we use the fact that the spectra of the same orbit with different deviations are different in the ordered case (Figs. 4(b) and 4(c)], while they are the same in the chaotic case (Figs. 6(b) and 6(c)].

The fact that the spectrum is invariant with respect to the initial orientation of the infinitesimal deviation ξ_0 for chaotic orbits, but not for ordered orbits, reflects a fundamental difference between these two kinds of motion. Two sets of initial conditions (\mathbf{x}_0, ξ_0) and (\mathbf{x}_0, ξ'_0) produce two different sequences (\mathbf{x}_i, ξ_i) and (\mathbf{x}_i, ξ'_i) , $i=1,2,3, \dots$. In the case of ordered orbits the two sequences are different for arbitrarily long times, but in the case of chaotic orbits the two sequences converge to a unique sequence after a time (number of iterations) t_c . (In our examples of Figs. 5 and 6, $t_c \approx 10^2$ and $t_c \approx 10^5$, respectively.)

For orbits exhibiting Arnold diffusion, there is a very slow convergence to a unique spectrum, but the time required is usually much larger than any realistic time scale (in Ref. [2], we found that in most cases $t_c > 10^{10}$ periods). Such orbits behave like ordered orbits with spectra depending on the initial orientation of ξ for all times of practical interest.

In our example of Fig. 6, the time $t=10^5$ is much shorter than 10^9 , but it is still somewhat long. This relatively long time is required because of the very small chaoticity of the orbit with $\beta=0.3051$ (the Lyapunov characteristic number is only $\mathcal{L}=4 \times 10^{-7}$).

In other cases, where chaos is stronger, the distinction between ordered and chaotic orbits can be found much faster. In a previous paper [10], we could distinguish ordered and chaotic domains after only $t=20-10$ iterations, by calculat-

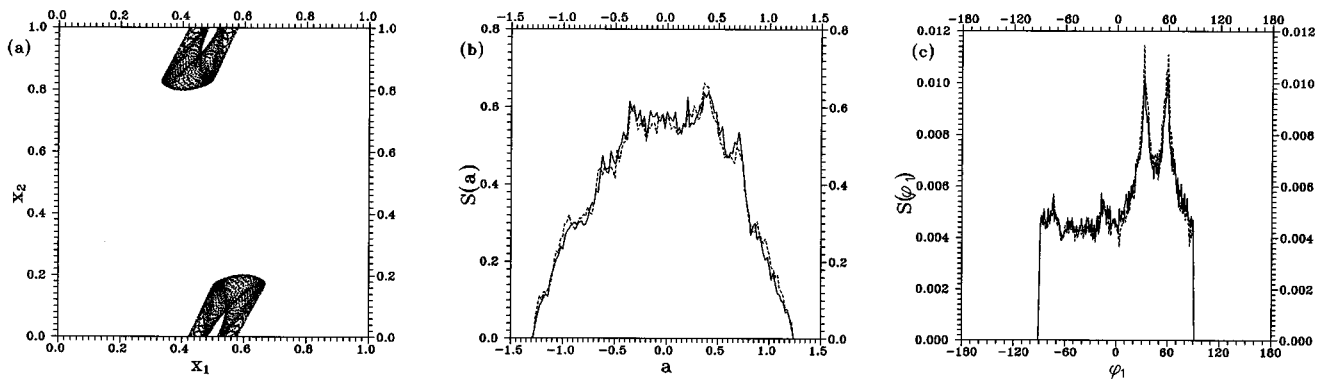


FIG. 6. (a)–(c) The same as in Figs. 4(a)–4(c) but with $\beta=0.3051$. Orbit (3) in this case is slightly chaotic. The two spectra in this figure are very close to each other.

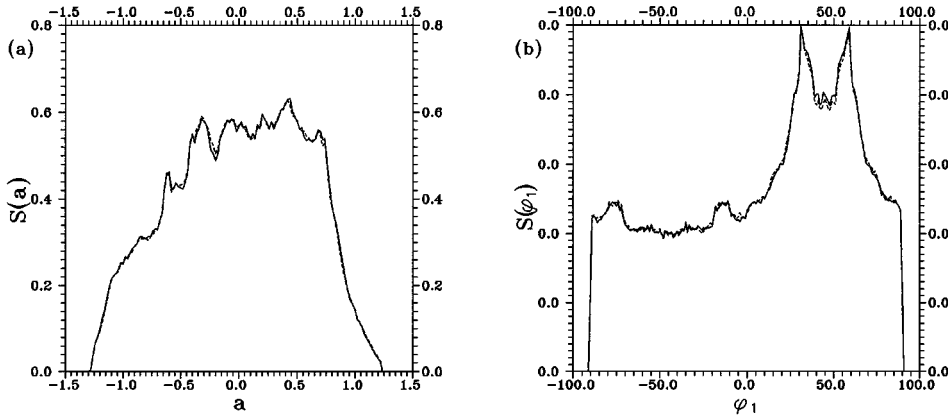


FIG. 7. The spectra of (a) stretching numbers and (b) helicity angles ϕ_1 of the (chaotic) orbit (3) with the same deviations as in Figs. 4 and 6, calculated for $t=2 \times 10^6$ iterations. The spectra are almost completely identical.

ing the average values of the stretching numbers $\langle a \rangle_t$ (short-time Lyapunov characteristic numbers) and helicity angles $\langle \phi \rangle_t$, for ten iterations after a transient interval of ten iterations. However, the distinction was based on the properties of *intervals* of ordered and chaotic orbits and not individual orbits. On the other hand, the new method refers to individual orbits and it is very efficient particularly in thin chaotic layers, where \mathcal{L} is very small.

Another method for distinguishing between ordered and chaotic orbits was developed by Laskar and co-workers [11,12]. This method performs a “frequency analysis” of the Fourier spectrum of an orbit. Ordered orbits have almost constant frequencies, while the frequencies of chaotic orbits vary in an irregular way, over time and space.

We have applied a fast Fourier transform with $N=2^{19}=524\,288$ periods at the beginning and at the end of 10^9 iterations of both the regular orbit ($K=3$, $\beta=0.1$) and the chaotic orbit ($K=3$, $\beta=0.3051$). No drift in the main frequencies was observed for both orbits up to an accuracy of 2×10^{-6} . A more accurate analysis, with the frequency analysis algorithm, after 10^9 periods, might give a change of the frequency by less than 2×10^{-6} . On the other hand our method distinguishes clearly the chaotic from the ordered case after less than 10^5 periods.

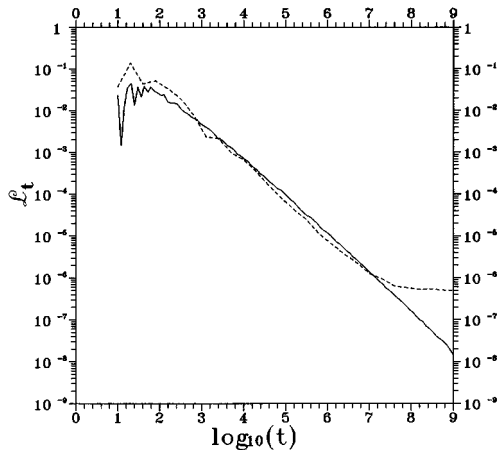


FIG. 8. The finite time Lyapunov characteristic numbers of two orbits with $K=3$ and the same initial conditions [those of orbit (3)], and the same initial deviations $z_1=z_2=z_3=z_4=1$, for $\beta=0.1$ (solid line) and 0.3051 (dashed line).

III. THEORETICAL EXPLANATION

We know that in 3D systems or 4D maps, ordered orbits lie on invariant 2D tori. The projection of such a torus on any 3D space of the 4D Poincaré surface of section is also a 2D torus.

An arbitrary initial deviation ξ_0 of an ordered orbit becomes tangent to the 2D torus after a few iterations. However, in general two different initial deviations ξ_0 and ξ'_0 lead to different sequences of deviations ξ_i and ξ'_i on the tangent planes at the points \mathbf{x}_i (Fig. 9). Thus the spectra are different. Only in exceptional cases the tangent vectors may happen to be approximately the same. In such cases another random initial deviation ξ'_0 would give a different sequence.

On the other hand, if an orbit is chaotic two arbitrary deviations ξ_0 and ξ'_0 give essentially the same spectra. This is due to the fact that the deviations ξ_i , after a short initial transient period, lie almost exactly along the dominant direction at each point. By “dominant direction” we mean the most frequent direction \mathbf{z}_i near each point \mathbf{x}_i of an orbit. This can be seen easily in a case of two dimensions (x_1, x_2) (i.e., $\beta=0$). Assume that the initial point \mathbf{x}_0 is along an unstable asymptotic curve (unstable manifold) of the standard map. Whatever the initial deviation ξ_0 , after a few iterations the deviations ξ_i are along the unstable asymptotic curve (Fig. 10). We see that near each point, say \mathbf{x}_i , there is a dominant helicity angle ϕ_i . However, in some regions (e.g., inside the small square of Fig. 10) we see some turning points, where

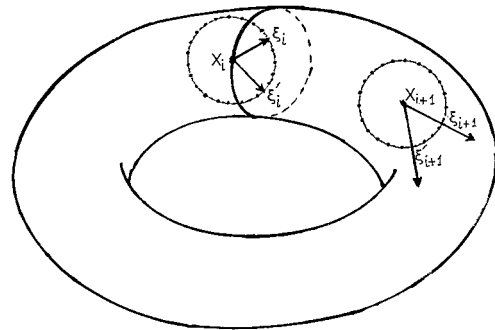


FIG. 9. The deviation ξ_0 from an ordered orbit becomes tangent to a 2D torus, after a few iterations, at successive points \mathbf{x}_i and \mathbf{x}_{i+1} (vectors ξ_i and ξ_{i+1}). A different initial deviation ξ'_0 from the same orbit gives in general different deviations ξ'_i and ξ'_{i+1} at the same points \mathbf{x}_i and \mathbf{x}_{i+1} .

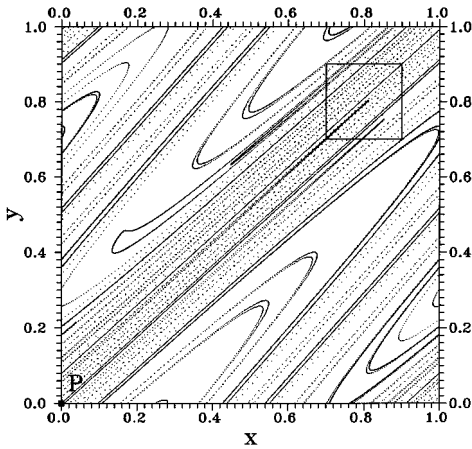


FIG. 10. The unstable asymptotic curve of the main periodic orbit ($x_1=x_2=0$) in map (3) for $K=10$ and $\beta=0$ fills the chaotic domain of the (x_1, x_2) plane. Note the turning points in the small square ($0.70 < x < 0.90$, $0.70 < y < 0.90$).

the direction of the unstable asymptotic curve changes continuously from ϕ_i to $180^\circ + \phi_i$, taking all intermediate values of the helicity angle ϕ . Such turning points appear everywhere in phase space if we calculate the unstable asymptotic curve long enough. During a long period the value of ϕ inside a small square takes all possible values from -180° to 180° , but most of the time it takes one dominant value. Thus the spectrum is characterised by the frequency of appearance of the *dominant* directions ϕ_i at successive points \mathbf{x}_i .

The unstable asymptotic curve of Fig. 10 passes arbitrarily close to every point of the chaotic domain. Therefore a different initial condition \mathbf{x}'_0 has its images \mathbf{x}'_i very close to

the same asymptotic curve of Fig. 10. Furthermore any deviation ξ'_0 from this orbit, after a short transient period, becomes parallel to the direction of the asymptotic curve closest to the point \mathbf{x}'_i . This means that we should have the same spectrum as that of an orbit starting at \mathbf{x}_0 . However, the sequence of helicity angles ϕ'_i (and stretching numbers a'_i) is different from that of \mathbf{x}_0 . This means that the time needed for the two spectra to agree closely may be somewhat long. But the convergence of two different deviations ξ_0 from the *same* orbit \mathbf{x}_i is much faster.

Similar considerations apply to systems of four dimensions. In this way we explain the fast agreement of the spectra of each orbit [e.g., orbits (1) or (2) in Fig. 3] with different initial deviations, but the slower convergence of the spectra of the different orbits [(1) and (2)] [compare Figs. 3(a), 3(c), and 3(d)]. The same arguments explain the fast convergence of \mathcal{L}_i in Fig. 2(b) for two different deviations from the *same* orbit, and the slower convergence of \mathcal{L}_i for two *different* orbits.

Thus we explain qualitatively the characteristics of the spectra in 4D maps. In particular, we explain the fundamental difference between the spectra of ordered orbits [Figs. 4(b) and 4(c)] and chaotic orbits [Figs. 6(b) and 6(c)]. *The spectra of stretching numbers and helicity angles of a given orbit, but different initial deviations, are different in the case of ordered orbits, while they are the same in the case of chaotic orbits.*

ACKNOWLEDGMENTS

This research was supported in part by the Greek General Secretariat for Research and Technology (PENED 293/1995). C. E. received support from the Greek Foundation of State Scholarships (I.K.Y.).

-
- [1] N. Voglis and G. Contopoulos, *J. Phys. A* **27**, 4899 (1994).
 - [2] G. Contopoulos and N. Voglis, *Celest. Mech. Dyn. Astron.* **64**, 1 (1996).
 - [3] J. S. Nicolis, G. Meyer-Kress, and G. Haubs, *Z. Naturforsch. A* **38**, 1157 (1983).
 - [4] H. Fujisaka, *Prog. Theor. Phys.* **70**, 1264 (1983).
 - [5] R. Benzi, G. Paladin, G. Parisi, and A. Vulpiani, *J. Phys. A* **18**, 2157 (1985).
 - [6] P. Grassberger, R. Badii, and A. Politi, *J. Stat. Phys.* **51**, 135 (1988).
 - [7] S. Udry and D. Pfenniger, *Astron. Astrophys.* **198**, 135 (1988).
 - [8] M. A. Sepulveda, R. Badii, and E. Pollak, *Phys. Rev. Lett.* **63**, 1226 (1989).
 - [9] C. Froeschlé, Ch. Froeschlé, and E. Lohinger, *Celest. Mech. Dyn. Astron.* **56**, 307 (1993).
 - [10] G. Contopoulos and N. Voglis, *Astron. Astrophys.* **317**, 73 (1997).
 - [11] J. Laskar, *Physica D* **67**, 257 (1993).
 - [12] J. Laskar, C. Froeschlé, and A. Celletti, *Physica D* **56**, 253 (1992).